J Mater Sci: Mater Med (2007) 18:857–864
DOI 10.1007/s10856-006-0083-0

# A novel bioactive porous bredigite ($Ca_7MgSi_4O_{16}$) scaffold with biomimetic apatite layer for bone tissue engineering

**Chengtie Wu · Jiang Chang · Wanyin Zhai · Siyu Ni**

Received: 16 August 2005 / Accepted: 27 January 2006 / Published online: 9 January 2007


**Abstract** The aim of this study was to develop a novel bioactive, degradable and cytocompatible bredigite ($Ca_7MgSi_4O_{16}$) scaffold with biomimetic apatite layer for bone tissue engineering. Porous bredigite scaffolds were prepared using polymer sponge method. The bredigite scaffolds with biomimetic apatite layer (BTAP) were obtained by soaking bredigite scaffolds in simulated body fluid (SBF) for 10 days. The porosity and in vitro degradability of BTAP scaffolds were investigated. In addition, osteoblast-like cell morphology, proliferation and differentiation on BTAP scaffolds were evaluated and compared with $\beta$-tricalcium phosphate ($\beta$-TCP) scaffolds. The results showed that BTAP scaffolds possessed 90% of porosity. The degradation of BTAP scaffolds was comparable to that of $\beta$-TCP scaffolds. Cells on BTAP scaffolds spread well and presented a higher proliferation rate and differentiation level as compared with those on $\beta$-TCP scaffolds. Our results indicated that BTAP scaffolds were degradable and possessed the function to enhance cell proliferation and differentiation, and might be used as bone tissue engineering materials.

C. Wu · J. Chang (✉) · W. Zhai · S. Ni
Biomaterials and Tissue Engineering Research Center, Shanghai Institute of Ceramics, Chinese Academy of Sciences, 1295 Dingxi Road, Shanghai 200050, P. R. China
e-mail: jchang@mail.sic.ac.cn

C. Wu
Graduate School of Chinese Academy of Sciences, 319 Yueyang Road, Shanghai 200050, P. R. China

## Introduction

Bone tissue engineering presents an alternative approach to the repair and regeneration of damaged bone tissue, avoiding the need for a permanent implant. Porous scaffolds in bone tissue engineering require three dimensionally interconnected porous structures. Such porous structure can provide sufficient space for cell adhesion, proliferation, differentiation and the ingrowth of new bone tissue. The bioactivity of scaffolds is important for stimulation of cell growth and differentiation, which benefits the regeneration of big size bone defect. Previous studies have shown that porous $\beta$-tricalcium phosphate ($\beta$-TCP) ceramic is essentially a bio-resorbable calcium phosphate material. Its tissue biocompatibility is excellent and it may act as a scaffold allowing bone regeneration and ingrowth [1, 2]. Furthermore, porous $\beta$-TCP scaffolds possess resorbable characteristic [3, 4] and are considered for bone tissue engineering applications [5]. However, $\beta$-TCP scaffolds can not stimulate cell growth on scaffolds, which is thought to be important for bone tissue engineering application, particularly in regeneration of big size bone defect.

Previous studies have shown that the Si and Ca containing bioactive glasses can stimulate cell proliferation [6]. In addition, bioactive glasses can induce the formation of bone-like apatite in vitro, which can enhance bone cell proliferation and differentiation [7–10]. Recently, studies have shown that some silicate ceramics, such as wollastonite and bredigite, possess similar bioactivity with bioactive glasses [11, 12]. The Si and Ca containing ionic products from bredigite dissolution could promote cell proliferation, and bredigite ceramics could induce bone-like apatite

formation in SBF [12]. These discoveries have stimulated our investigation on porous bredigite as scaffolds for bone tissue engineering. The aim of this study was to prepare bioactive porous bredigite scaffolds with biomimetic apatite layer for bone tissue engineering.

## Materials and methods

### Preparation of bredigite scaffolds

Bredigite powders were prepared by sol-gel process using tetraethyl orthosilicate ($(C_2H_5O)_4Si$, TEOS), magnesium nitrate hexahydrate ($Mg(NO_3)_2{\cdot}6H_2O$) and calcium nitrate tetrahydrate ($Ca(NO_3)_2{\cdot}4H_2O$) as raw materials (mol ratio: TEOS/$Mg(NO_3)_2{\cdot}6H_2O$/$Ca(NO_3)_2{\cdot}4H_2O$ = 4:1:7). TEOS was mixed with water and 2 M $HNO_3$ and hydrolyzed for 30 min under stirring. Then, the $Mg(NO_3)_2{\cdot}6H_2O$ and $Ca(NO_3)_2{\cdot}4H_2O$ were added into the mixture, and reactants were stirred for 5 h at room temperature. After the reaction, the solution was maintained at 60°C for 1 day and dried at 120°C for 2 days to obtain dry gel. The dry gel was calcined at 1150°C for 3 h with a heating rate of 2°C/min to obtain bredigite powders. Bredigite powders were suspended in polyvinyl alcohol aqueous solution (PVA, 10 wt.%) and stirred in a glass beaker to obtain well-dispersed slurry. The ratio of powder mass to PVA solution mass was 1/1. Polyurethan foam template (density 25 ppi, porosity >97%, No. 6 Plastic Works, Shanghai) was cut into the desired shape and size and the prepared sponge was immersed in the glass beaker containing bredigite slurry and compressed with glass stick to force the bredigite slurry to migrate into the pores of the foams. The struts of the foams were uniformly coated with ceramic slurry while the pores were maintained open. Then, the impregnated forms were dried at 60°C, heated at 300°C for 1 h to remove the polymeric struts and then sintered at 1350°C for 3 h at a heating rate of 1°C/min. The sintered bredigite scaffolds were characterized by X-ray diffraction (XRD, Geigerflex, Rigaku Co., Japan) with a step size of 0.02° at a scanning rate of 10°/min in the $2\theta$ range of 10–60° and observed by scanning electron microscopy (SEM; JSM-6700F, JEOL, Tokyo, Japan). $\beta$-TCP porous scaffolds were prepared using the same method and sintered at 1200°C for 3 h as the controls.

### Biomimetic modification of bredigite scaffolds

The simulated body fluid (SBF) was prepared according to the method described by Kokubo [13]. Briefly, reagent-grade $CaCl_2$, $K_2HPO_4{\cdot}3H_2O$, NaCl, KCl, $MgCl_2{\cdot}6H_2O$, $NaHCO_3$, and $Na_2SO_4$ were dissolved in distilled water and pH was adjusted with tris-(hydroxymethyl)-aminomethane [$(CH_2OH)_3CNH_2$] and hydrochloric acid (HCl). The ion concentrations were similar to those in human blood plasma as shown in Table 1. Bredigite scaffolds were soaked in SBF (pH 7.40) at 37°C for 10 days, and the ratio of solution volume to scaffold mass was 200 ml/g. After soaking, the scaffolds was dried at 120°C for 1 day and the bredigite scaffolds with biomimetic apatite layer (BTAP) were obtained.

**Table 1** Ion concentrations of SBF and human blood plasma (mM)

| | $Na^+$ | $K^+$ | $Mg^{2+}$ | $Ca^{2+}$ | $Cl^-$ | $HCO_3^-$ | $HPO_4^{2-}$ |
|---|---|---|---|---|---|---|---|
| SBF | 142.0 | 5.0 | 1.5 | 2.5 | 148.8 | 4.2 | 1.0 |
| Blood plasma | 142.0 | 5.0 | 1.5 | 2.5 | 103.0 | 27.0 | 1.0 |

### Characterization of BTAP scaffolds

The obtained BTAP scaffolds were characterized by XRD and SEM coupled with energy dispersive spectrometer (EDS, INCA Energy, Oxford Instruments, UK). The porosity of BTAP and $\beta$-TCP scaffolds was measured according to Archimedes' principle described by Ozgür Engin and Cüneyt Tas [14]. Samples with a size of $6 \times 6 \times 4$ mm$^3$ were used for the measurement and water was used as liquid medium. The porosity (P) was calculated according to the following formulation $P = (W_2–W_1)/(W_2–W_3) \times 100\%$, where $W_1$ is the weight of the sample in air, $W_2$ is the weight of the sample with water, and $W_3$ is the weight of the sample suspended in water. The compressive strength of the scaffolds was measured using a universal testing machine (AG-5KNL, Shimadzu Co., Japan) at a cross-head speed of 0.5 mm/min.

For evaluation of degradation, BTAP and $\beta$-TCP scaffolds were soaked in Ringer's solution (pH 7.40) at 37°C in shaking water bath for 6 h, 1, 3, 7 14 and 28 days, respectively, and the solution was refreshed every day. The ratio of solution volume to scaffolds mass was 200 ml/g. After the set soaking time, the scaffolds were dried at 120°C for 1 day, and the final weight of each sample was accurately measured. The weight loss was expressed as percentage of the initial weight.

### Cell culture

Osteoblast-like cells were isolated from calvaria of neonatal (less than 2 days old) Sprague-Dawley rats by an enzymatic digestive process as described previously

[15, 16]. Briefly, the rat calvaria were washed three times in phosphate-buffered saline (PBS, pH = 7.4) and then minced into fragments about 1 mm in diameter. After washing the bone fragments three times with PBS, the chips of calvaria were digested for 20 min at 37°C with 0.25% (w/v) trypsin-EDTA solution (Gibco, USA) to diminish fibroblastic contamination. Then the samples were treated with 1 mg/ml collagenase (Sigma) at 37°C for 90 min to release osteoblast-like cells from the calvaria. The supernatants were centrifuged at 1000 rpm for 10 min, and then suspended in the RPMI 1640 (Roswell Park Memorial Institute 1640) medium (Gibco, USA) containing 15% (v/v) heat-inactivated fetal calf serum with 50 μg/ml L-ascorbic acid, 1% glutamine, 50 UI/ml penicillin/streptomycin, and incubated in a 75 $cm^2$ flask at 37°C under a humidified atmosphere consisting of 5% $CO_2$. Culture media were refreshed every 2 days until the cells reached confluency. The cells were routinely subcultured by trypsinization [0.05% (w/v) trypsin and 0.02% (w/v) EDTA in PBS], and the cells used in the study were between second and fourth passages.

### Cell culture on the scaffolds

The cells ($1.0 \times 10^5$) were seeded on each BTAP scaffold ($6 \times 6 \times 4$ mm) in a 48-well plate and incubated for 1, 3, 7 and 14 days in DMEM culture medium supplemented with 15% FCS maintained at 37°C in a humidified atmosphere of 95% air and 5% $CO_2$. After different culture time, the scaffolds were removed from the culture wells, rinsed with PBS. For SEM observation, the cells on the scaffolds were fixed with 2.5% glutaraldehyde, dehydrated in a grade ethanol series (30, 50, 70, 90 and 96% (v/v)) for 10 min respectively with final dehydration in absolute ethanol twice followed by drying in hexamethyldisilizane (HMDS) ethanol solution series [17]. The MTT (3-(4,5-dimethylthiazol-2-yl)-2,5-diphenyl tetrazolium bromide) test was used for the evaluation of cell proliferation on the scaffolds. After different culture time, the scaffolds were incubated in a MTT solution at 37°C for 4 h. After removal of the supernatants, dimethyl sulfoxide (DMSO) was added to each well to completely dissolve the purple formazan. The optical density (OD) of each well was measured at 590 nm using an enzyme-linked immunoadsorbent assay (ELISA) plate reader (EL × 800, BIO-TEK, USA). For evaluation of alkaline phosphate activity (ALP), the cells on the scaffolds were lysated with a solution containing 0.1% Triton X-100 after different culture time and ALP activity was assayed by the method of Lowry [18]. Aliquotes of cell lysates were incubated with reaction solution (containing 2-amino-2-mehtyl-1-propanol, $MgCl_2$, and *p*-nitrophenylphosphate) at 37°C for 30 min. The conversion of *p*-nitrophenylphosphate to *p*-nitrophenol was stopped by adding NaOH [19], and the absorbance at 405 nm was measured with a spectrophotometer (UV-Vis 8500, Shanghai). The ALP activity (expressed as nanomoles of converted *p*-nitrophenol/min) was normalized by total intracellular protein content and expressed as nanomoles of converted *p*-nitrophenol/min/mg proterin. The prepared *β*-TCP porous scaffolds were used as the controls for cell proliferation and diffentiation.

### ICP-AES measurement

After 7 days of cell culture, BTAP and *β*-TCP scaffolds were taken out and Ca, Mg, P and Si ion concentrations in the culture medium were measured by inductively coupled plasma atomic emission spectroscopy (ICP-AES; Varian Co., USA).

### Statistical analysis

All data were expressed as means ± standard deviation (SD) for $n = 6$ and were analyzed using One-Way ANOVA with a Post Hoc test. A $p$-value $<0.05$ was considered statistically significant.

## Results

### Characterization of the scaffolds

The XRD pattern of the bredigite scaffolds sintered at 1350°C for 3 h is shown in Fig. 1. It was obvious that

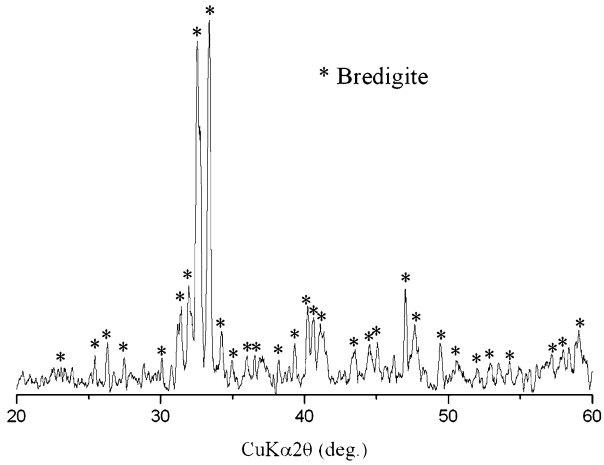


**Fig. 1** XRD pattern of bredigite scaffolds sintered at 1350°C for 3 h

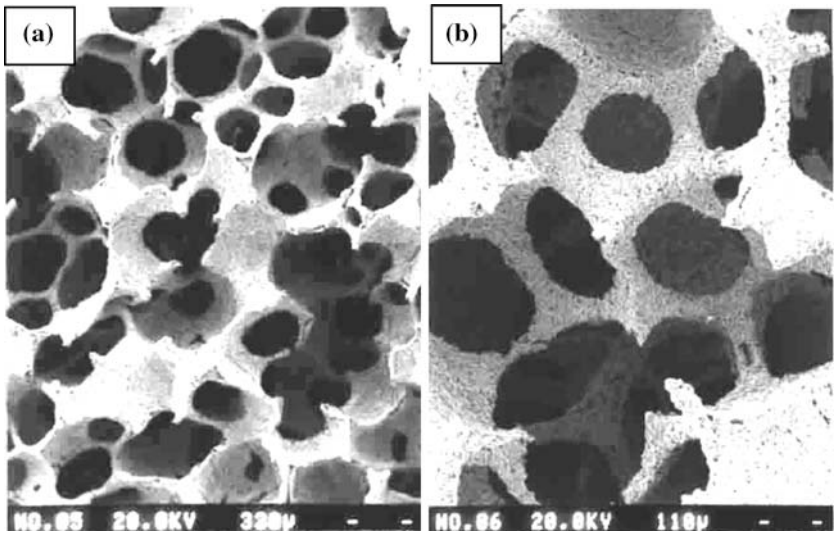


**Fig. 2** SEM micrographs of bredigite scaffolds sintered at 1350°C for 3 h

only bredigite peaks existed in the pattern (JCPD 27–1060) indicating a pure breidigite scaffold. The morphology and structure of the as-fabricated bredigite porous scaffolds are shown in Fig. 2. The pores in the scaffolds were completely interconnected (Fig. 2a). The higher magnification SEM micrograph showed that the size of the pores was about 300–500 μm and the thickness of pore wall was about 60–100 μm (Fig. 2b).

The XRD pattern of BTAP scaffolds was shown in Fig. 3, and it was obvious that apatite peaks (JCPD 24–0033) appeared. The morphological features of the BTAP scaffolds were presented in Fig. 4. It was clear to see that an apatite layer was formed on the wall of the scaffolds (Fig. 4a). The high magnification SEM micrograph showed that the size of the apatite crystals was about 100 nm (Fig. 4b). The corresponding EDS analysis revealed that the Ca/P ratio of the apatite layer was about 1.61 (Fig. 4c). The porosity of BTAP scaffolds prepared with this method is about 90%. The corresponding compressive strength of the scaffolds was listed in Table 2. It is clear to see that the compressive strength of BTAP scaffolds (101 kPa) was lower than the pure bredigite scaffolds (233 kPa), but it was still higher than that of $\beta$-TCP scaffolds (50 kPa) prepared by the same method.

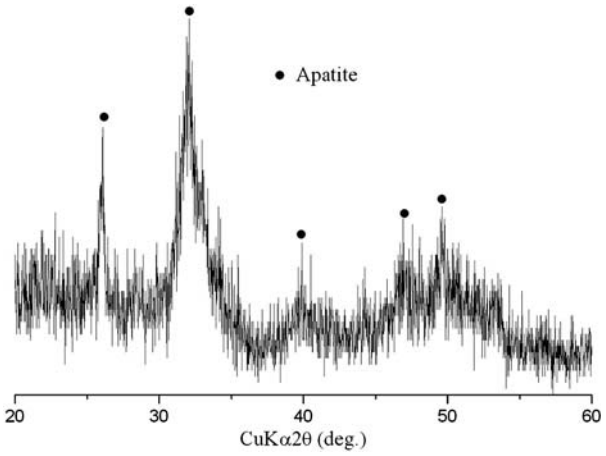


**Fig. 3** XRD pattern of BTAP scaffolds. Biomimetic apatite layer was formed on the surface of BTAP scaffolds

The weight loss of BTAP scaffolds in Ringer's solution is presented in Fig. 5. It could be seen that the weight loss of BTAP scaffolds increased with the increase of soaking time and was comparable to that of $\beta$-TCP scaffolds, which indicated that BTAP scaffolds were soluble in Ringer's solution.

## Cell morphology on BTAP scaffolds

Cell morphology on BTAP scaffolds was examined by SEM. After 1 day of culture, cells attached on BTAP scaffolds (Fig. 6a), and the attached cells mainly presented a close contact with the surface and adopted an extended morphology with numerous filopodia (Fig. 6b). After 7 days of culture, the cells on BTAP scaffolds showed a spread appearance (Fig. 6c and d). After 14 days of culture, the cells on BTAP scaffolds almost formed a layer and presented an elonged and smooth morphology (Fig. 6e and f).

## Cell proliferation and differentiation on BTAP scaffolds

MTT tests showed that cells on two scaffolds proliferated obviously with the increase of culture time (Fig. 7). However, cells on BTAP scaffolds presented

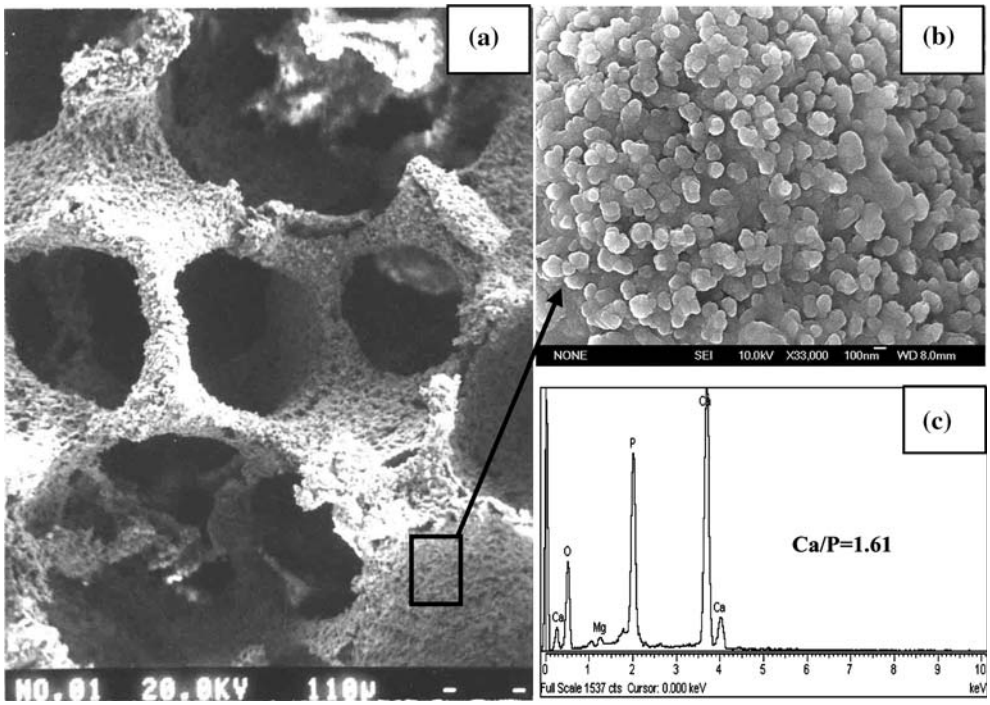


**Fig. 4** SEM and EDS analysis of BTAP scaffolds. The Ca/P of apatite on the surface of scaffolds was 1.61

**Table 2** The compressive strength of bredigite, BTAP and $\beta$-TCP scaffolds

| Scaffolds | Bredigite | BTAP | $\beta$-TCP |
|---|---|---|---|
| Compressive Strength (kPa) | 233 ± 14 | 101 ± 8 | 50 ± 20 |

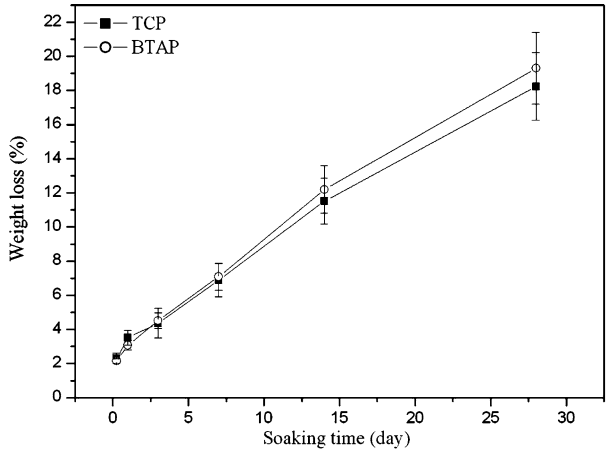


**Fig. 5** The weight loss of BTAP and $\beta$-TCP scaffolds in Ringer's solution for different time periods

a higher proliferation rate ($p < 0.05$) as compared with those on $\beta$-TCP scaffolds after 7 days of culture. ALP activity was used as an early marker for cell differentiation on scaffolds. Figure 8 illustrates the changes of ALP activity of cells on day 3 and day 7 of culture. It could be seen that ALP levels increased for both BTAP and $\beta$-TCP scaffolds with the increase of culture time, and the cells on BTAP scaffolds presented a higher ALP activity than those on $\beta$-TCP scaffolds ($p < 0.05$).

### ICP-AES measurement

The ionic concentrations of the culture medium are listed in Table 3. Generally, BTAP scaffolds released a higher level of Si and Mg ions compared with $\beta$-TCP scaffolds. The Ca and P concentrations of BTAP scaffolds in culture medium were similar with those of the $\beta$-TCP scaffolds.

## Discussion

This study was undertaken to fabricate bredigite scaffolds by polymer sponge method. The prepared bredigite scaffolds possess highly porous structure with large pore size (300–500 μm). BTAP scaffolds were obtained by soaking bredigite scaffolds in SBF. This biomimetic process mimics biomineralization and leads to the formation of a bone-like apatite layer on scaffold surface. The obtained BTAP scaffolds possess high porosity (90%) and pore interconnectivity. Previously, El-Ghannam et al. prepared porous bioactive glasses with polyethylene glycol as porogens, however, the pore size is about 10–160 μm and porosity is only 36%, which might be to low for tissue engineering

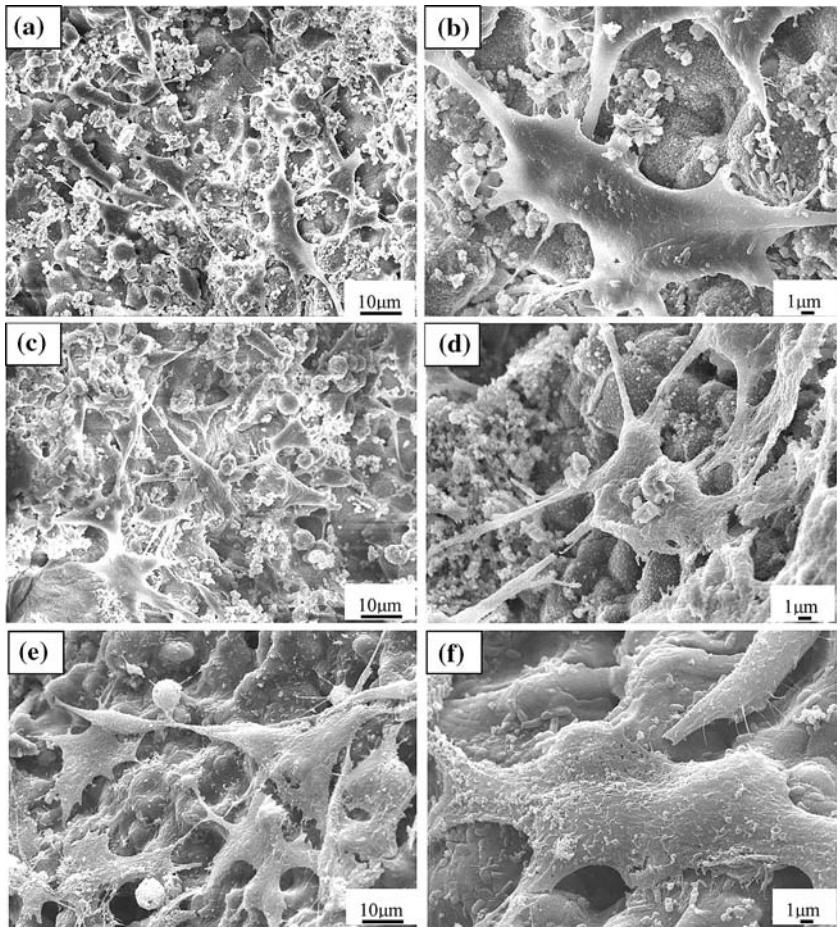


**Fig. 6** Osteoblast-like cell morphology on BTAP scaffolds after culturing for 1, 7 and 14 days. (**a**) and (**b**) 1d, (**c**) and (**d**) 7d, (**e**) and (**f**) 14d

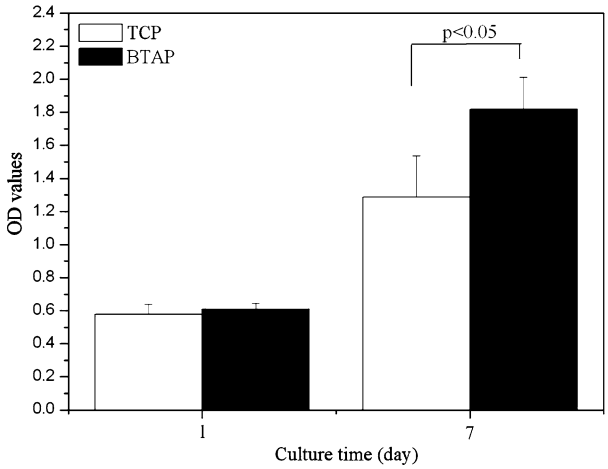


**Fig. 7** Osteoblast-like cell proliferation on BTAP and $\beta$-TCP scaffolds. OD value on Y-axis represents the number of living cells

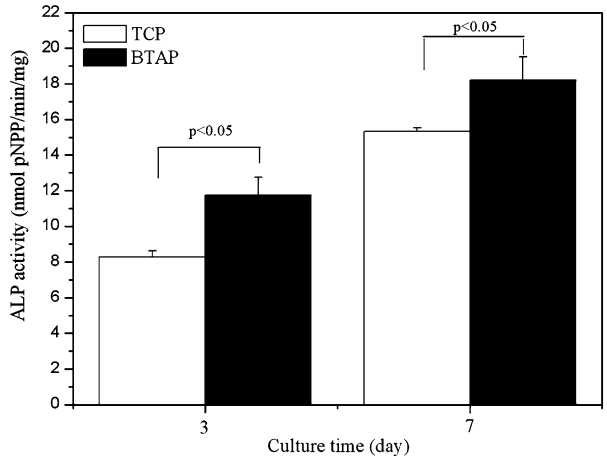


**Fig. 8** Alkaline phosphatase activity of osteoblasts-like cells cultured on BTAP and $\beta$-TCP scaffolds for 3 and 7 days

applications [20]. Although Jones et al. improved the interconnectivity of porous bioactive glasses using foaming method, the size of open pores was only about 100 μm and pore distribution was not regular [21]. In contrast, the polymer sponge method produces highly interconnected porous ceramic scaffolds with high porosity through replication of porous polymer sponge templates [22]. In our study, the porous BTAP scaffolds prepared by polymer sponger method pos-

**Table 3** Ion concentrations of culture medium after 7 days of culture (mM)

| Scaffolds | Ca | Mg | *P* | Si |
|---|---|---|---|---|
| $\beta$-TCP | 1.94 | 0.20 | 0.87 | 0 |
| BTAP | 1.83 | 0.67 | 0.77 | 1.59 |

sessed improved pore structure and interconnectivity as compared with porous bioactive glasses. The high porosity of the BTAP scaffolds is expected to be sufficient to permit tissue ingrowth and blood and nutrients supply [23]. Furthermore, the appropriate pore size of 300–500 μm can enhance the diffusion of nutrients into the 3-D scaffolds [23]. Although the mechanical strength of BTAP scaffolds was lower as compared with pure bredigite scaffolds, it was still higher than that of $\beta$-TCP scaffolds (50 kPa) prepared by the same method and the scaffolds still maintained an integrated appearance and could be handed easily for cell incorporation. In bone tissue engineering applications, the scaffolds mainly provide the initial mechanical support for cells, so their ease of handling during cell incorporation is critical. Our results showed that the BTAP scaffolds could meet the requirements as cell carrier.

The degradation of the scaffolds can provide room for matrix deposition and tissue growth [5], which is important for bone tissue engineering applications. It is known that dissolubility can be considered as one factor of biodegradation, and dissolution mainly affect the biodegradation of ceramics [24]. In our study, the BTAP scaffolds revealed an obvious dissolution in balanced salt solution and the dissolution was comparable to that of porous $\beta$-TCP scaffolds. Our result suggests that BTAP scaffolds may possess similar degradability as porous $\beta$-TCP scaffolds. However, further study is needed to confirm the in vivo degradability of BTAP scaffolds.

Examination of cell morphology, proliferation and differentiation were carried out to evaluate the cell behavior on BTAP scaffolds. In general, cells adhered and spread well on BTAP scaffolds as confirmed by their spreading morphologies. In addition, cells on the BTAP scaffolds showed a higher proliferation rate and differentiation level as compared with $\beta$-TCP scaffolds. $\beta$-TCP is a well-known degradable bioceramic, which has been used as bone defect filling materials and considered as porous scaffolds for bone tissue engineering applications. In comparison to $\beta$-TCP, our results indicated that BTAP scaffolds had the function to enhance cell proliferation and differentiation within scaffolds and might be suitable for tissue engineering applications. There are two main factors that may affect cell behavior on BTAP scaffolds. One is the ionic products from scaffolds which may stimulate cell proliferation and differentiation. We have found that the Mg and Si concentrations in culture medium containing BTAP were obviously higher than those in culture medium containing $\beta$-TCP. Previous studies have shown that Mg and Si could promote cell proliferation and differentiation [6, 25, 26]. Therefore, we believe that Mg and Si ions released from BTAP scaffolds play an important role in the stimulation of cell proliferation and differentiation, which is in accordance with previous findings on the role of Si containing ionic products from bioactive glasses [6, 27]. Secondly, the biomimetic apatite layer on the scaffolds might benefit cell spreading, proliferation and differentiation. Previously, extensive investigations have confirmed that bone-like apatite layer possessed the capacity to enhance the osteoblastic activity [7–10, 28]. Labat and Ohgushi et al. have found that the bone-like apatite layer possessed good binding ability with serum proteins and growth factors, which could stimulate cell proliferation and activate cell differentiation [29, 30]. In addition, Webster et al. found that nano-structured ceramics could enhance function of osteoblasts [31]. In a recent study, Chou et al. found that the morphology and structure of biomimetic apatite affected osteoblast viability, proliferation and gene expression [32]. In our study, the biomimetic apatite on BTAP scaffolds consisted of spherical crystals with nano-size structure, and the nano-apatite structure might have an active effect on cell behavior.

## Conclusions

In conclusion, porous bredigite scaffolds with high porosity and pore interconnectivity were prepared using polymer sponge method, and the bredigite scaffolds with biomimetic apatite layer were obtained by soaking bredigite scaffolds in SBF. Compared with $\beta$-TCP scaffolds, cells on BTAP scaffolds showed a higher cell proliferation rate and differentiation level. Our results indicate that bredigite scaffolds with biomimetic apatite layer are degradable, support cell attachment and stimulate cell proliferation and differentiation, and may be used as scaffolds for bone tissue engineering applications.

**Acknowledgments** This work is supported by the National Basic Science Research Program of China (973 Program) (Grant No: 2005CB522704) and Science and Technology Commission of Shanghai Municipality (Grant No: 05JD14005).

## References


1. K. KURASHINA, H. KURITA, Q. WU, A. OHTSUKA, H. KOBAYASHI, *Biomaterial* **13** (2002) 407
2. M. SATIO, H. SHIMIZU, M. BEPPU, M. TAKAGI, *J. Orthop. Sci.* **5** (2000) 275
3. K. OHURA, M. BOHNER, P. HARDOUIN, J. LEMAITRE, G. PASQUIER, B. FLAUTRE, *J. Biomed. Mater. Res.* **30** (1996) 193
4. K. OHSAWA, M. NEO, H. MATSUOKA, H. AKIYAMA, H. ITO, H. KOHNO, T. NAKAMURA, *J. Biomed. Mater. Res.* **52** (2000) 460
5. K. J. BURG, S. PORTER, J. F. KELLAM, *Biomaterials* **21** (2000) 2247
6. P. VALERIO, M. M. PEREIRA, A. M. GOES, M. F. LEITE, *Biomaterials* **25** (2004) 2941
7. A. EL-GHANNAM, P. DUCHEYNE, I. M. SHAPIRO, *J. Biomed. Mater. Res*. **29** (1995) 359
8. A. EL-GHANNAM, P. DUCHEYNE, I. M. SHAPIRO, *J. Biomed. Mater. Res*. **36** (1997) 167
9. C. LOTY, J. M. SAUTIER, H. BOULEKACHE, T. KOKUBO, H. M. KIM, *J. Biomed. Mater. Res*. **49** (2000) 423
10. N. OLMO, A. I. MARTÍN, A. J. SALINAS, J. TURNAY, V. R. MARÍA, M. A. LIZARBE, *Biomaterials* **24** (2003) 3383.
11. P. SIRIPHANNON, S. HAYASHI, A. YASUMORI, K. OKADA, *J. Mater. Res*. **14** (1999) 529
12. C. T. WU, J. CHANG, J. Y. WANG, S. Y. NI, W. Y. ZHAI, *Biomaterials* **26** (2005) 2925
13. T. KOKUBO, *J. Non-Cryst. Solids*. **120** (1990) 138
14. N. OZGÜR ENGIN, A. CÜNEYT TAS, *J. Eur. Ceram. Soc*. **19** (1999) 2569
15. C. G. BELLOWS, J. E. AUBIN, J. N. M. HEERSCHE, M. E. ANTOSZ, *Calcif Tissue Int*. **38** (1986) 143
16. S. L. ISHAUG, M. J. YASZEMSKI, R. BIZIOS, A. G. MIKOS, *J. Biomed. Mater. Res*. **28** (1994) 1445
17. R. A. HIRST, H. YESILKAYA, E. CLITHEROE, A. RUTMAN, N. DUFTY, T. J. MITCHELL, C. O. CALLAGHAN, P. W. ANDREW, *Infect. Immu.* **70** (2002) 1017
18. O. H. LOWRY, N. R. ROBERTS, M. WU, W. S. HIXTON, E. J. CRAWFORD, *J. Biol. Chem*. **207** (1954) 19
19. M. LIEBERHERR, I. VREVEN, G. VAES, *Biochem. Biophys. Acta*. **293** (1973) 160
20. A. EL-GHANNAM, P. DUCHEYNE, I. M. SHAPIRO, *J. Biomed. Mater. Res*. **29** (1995) 359
21. J. R. JONES, L. L. HENCH, *J. Biomed. Mater. Res. Part B: Appl. Biomater*. **68** (2004) 36
22. Y. ZHANG, M. ZHANG, *J. Biomed. Mater. Res*. **61** (2002) 1
23. D. W. HUTMACHER, *Biomaterials* **21** (2000) 2529
24. J. X. LU, M. DESCAMPS, J. DEJOU, G. KOUBI, P. HARDOUIN, J. LEMAITRE, J. P. PROUST, *J. Biomed. Mater. Res*. **63** (2002) 408
25. C. C. LIU, J. K. YEH, J. F. ALOIA, *J. Bone Mineral Res*. **3** (1988) 104
26. D. M. REFFITT, N. OGSTON, R. JUGDAOHSINGH, H. F. CHEUNG, B. A. EVANS, R. P. THOMPSON, J. J. POWELL, G. N. HAMPSON, *Bone* **32** (2003) 127
27. I. D. XYNOS, A. J. EDGAR, L. D. K. BUTTERY, L. L. HENCH, J. M. POLAK, *J. Biomed. Mater. Res*. **55** (2001) 151
28. J. E. G. HULSHOFF, K. VON DIJK, J. E. RUIJER, F. J. R. RIETVELD, L. A. GINSEL, J. A. JANSEN, *J. Biomed. Mater. Res*. **40** (1998) 464
29. B. LABAT, A. CHAMSON, J. FREY, *J. Biomed. Mater. Res*. **29** (1995) 1397
30. H. OHGUSHI, Y. DOHI, T. YOSHIKAWA, S. TAMAI, S. TABATA, K. OKUNAGA, T SHIBUYA, *J. Biomed. Mater. Res*. **32** (1996) 341
31. T. J. WEBSTER, C. ERGUN, R. H. DOREMUS, R. W. SIEGEL, R. BIZIOS, *Biomaterials* **21** (2000) 1803
32. Y. F. CHOU, W. B. HUANG, J. DUNN, T. A. MILLER, B. M. WU, *Biomaterials* **26** (2005) 285